Proceedings of the VI National Conference of Neutron Scattering, Chlewiska, Poland, June 14–18, 2009

Magnetic Properties of RSn_2 (R = Tb, Dy) Compounds

A. Szytuła[a], D. Kaczorowski[b], Ł. Gondek[c], J. Czub[d] and K. Nenkov[e,f]

[a]M. Smoluchowski Institute of Physics, Jagiellonian University, Reymonta 4, 30-059 Kraków, Poland

[b]W. Trzebiatowski Institute of Low Temperature and Structure Research, Polish Academy of Sciences P.O. Box 1410, 50-950 Wrocław, Poland

[c]Faculty of Physics and Applied Computer Science, AGH University of Science and Technology al. Mickiewicza 30, 30-059 Kraków, Poland

[d]Faculty of Metal Engineering and Industrial Computer Science, AGH University of Science and Technology al. Mickiewicza 30, 30-059 Kraków, Poland

[e]Leibnitz-Institute for Solid State and Materials Research, P.O. Box 270116, D-01171 Dresden, Germany

[f]International Laboratory of High Magnetic Fields and Low Temperatures, Gajowicka 95, 53-529 Wrocław, Poland

Polycrystalline samples of $TbSn_2$ and $DySn_2$ were studied by means of magnetic susceptibility, electrical resistivity and heat capacity measurements. Both compounds have been found to order antiferromagnetically at low temperatures with some extra features in the ordered state due to changes in their magnetic structures. The two stannides exhibit metallic conductivity. The estimated crystal field levels splitting of Tb^{3+} and Dy^{3+} ground multiplets do not exceed 75 K.

PACS: 75.40.−s, 75.30.Kz, 72.15.Eb

1. Introduction

The binary RSn_2 stannides crystallise in the orthorhombic $ZrSi_2$-type structure (space group *Cmcm*), in which all the atoms occupy the 4c positions with different positional parameters [1]. Up to date no information was reported in the literature on the magnetic behaviour in $TbSn_2$. The compound $DySn_2$ was briefly studied as a part of investigation of the $DyFe_xSn_{2-x}$ system [2]. It was communicated to order magnetically at about 18 K, and to exhibit in the paramagnetic region an effective magnetic moment of 8.0 μ_B that is much less than the value expected for a trivalent Dy ion. The difficulties in obtaining monophased samples is probably the limiting factor in investigation of RSn_2 magnetic properties [3]. In this paper we report on the magnetic, electrical, transport, and thermodynamic properties of the two compounds, studied in a broad range of temperature.

2. Experimental

Polycrystalline samples of $TbSn_2$ and $DySn_2$ were synthesised by arc melting constituent elements of high purity (99.9% for rare earth and 99.99% for Sn) in argon atmosphere. The ingots were remelted several times in order to ensure good homogeneity. Subsequently, the products were sealed into evacuated quartz tubes and annealed at 900 °C for 10 days.

Purity of the samples was checked by means of X-ray powder diffraction. In both cases analysis of the X-ray pattern yielded the expected $ZrSi_2$-type structure for the main phase, and revealed very small contamination by some spurious phases (less than 5%). The latter could not be identified, however simple elements as well as their oxides were excluded, except the Tb_2O_3 phase.

Magnetic studies were carried in the 1.7–400 K temperature range and in magnetic field up to 50 kOe using a Quantum Design MPMS-5 SQUID magnetometer. The electrical resistivity was measured in the 4.2–300 K temperature range employing a standard DC four-points technique. Heat capacity measurements were performed in the 1.9–300 K temperature interval using relaxation method implemented in a Quantum Design PPMS platform.

3. Experimental results and discussion

3.1. Magnetic properties

The obtained magnetic data for $TbSn_2$ and $DySn_2$ are presented in Fig. 1. For both compounds, above roughly 50 K, the magnetic susceptibility obeys the Curie–Weiss law. The derived effective magnetic moment, μ_{eff}, amounts to $9.68(1)\mu_B$ and $10.39(1)\mu_B$ for the former and the latter stannide, respectively, in a very good agreement with the values expected for the free Tb^{3+} and Dy^{3+} ions. The paramagnetic Curie temperature, θ_p, is equal to −41.0(3) K and −27.2(2) K for $TbSn_2$ and $DySn_2$, respectively. The negative signs of θ_p hint at antiferromagnetic correlations between the Tb and Dy magnetic moments.

At low temperatures, the magnetic susceptibility data reveals long-range magnetic ordering in both compounds.

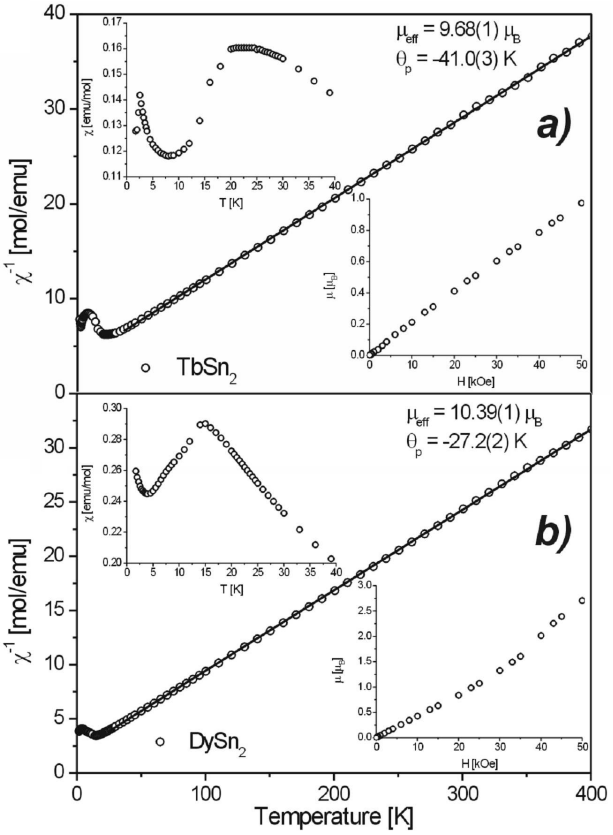

Fig. 1. Temperature dependences of the inverse molar magnetic susceptibility of $TbSn_2$ (a) and $DySn_2$ (b). The solid lines represent the Curie–Weiss fits discussed in the text. The upper insets show the magnetic susceptibility at the lowest temperatures studied. The lower insets display the dependence of the magnetic field variations on the magnetic moment measured at 1.7 K.

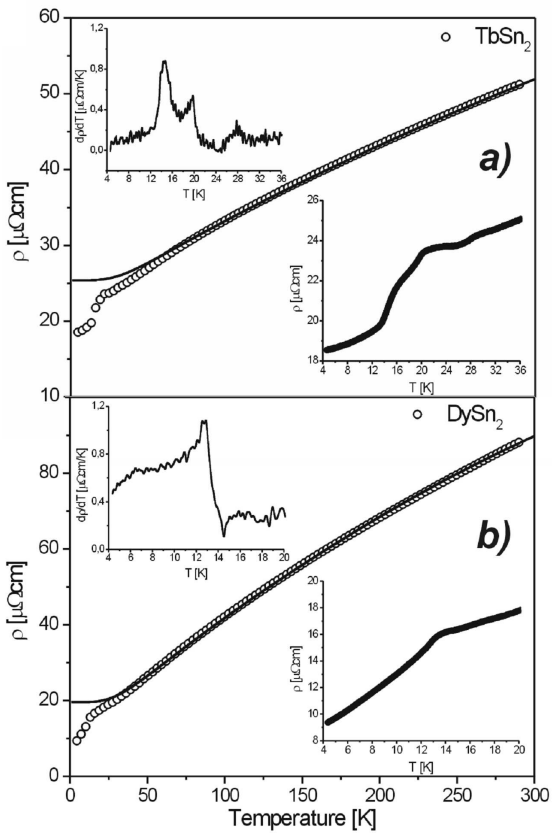

Fig. 2. Temperature variations of the electrical resistivity of $TbSn_2$ (a) and $DySn_2$ (b). The solid lines represent the BGM fits discussed in the text. The lower insets show the resistivity at the lowest temperature studied, while the upper insets display the corresponding temperature derivatives of the resistivity.

For $TbSn_2$, a broad hump in $\chi(T)$ around 22 K is visible, whereas a rather sharp susceptibility maximum at 15 K is evident for $DySn_2$ (see the upper insets to Fig. 1). In the ordered region, $\chi(T)$ shows some additional features, a spiky peak at 2.5 K in $TbSn_2$ and an upturn below 3 K in $DySn_2$ being the most pronounced ones. The 2.5 K anomaly for $TbSn_2$ seems to be due to Tb_2O_3 spurious phase.

The magnetization isotherms measured at 1.7 K, displayed in the lower insets to the Fig. 1, corroborate the antiferromagnetic character of the ground states in both compounds. Particularly, the isotherm taken for the Dy-based sample exhibits a clear metamagnetic-like transition near 30 kOe.

3.2. Electrical transport

In Fig. 2 the temperature variations of the electrical resistivity of $TbSn_2$ and $DySn_2$ are shown. Both materials exhibit typical metallic-like $\rho(T)$ dependences. Above 50 K, where the spin disorder resistivity may be considered to be temperature independent (i.e. crystal field effects are negligible, in line with the magnetic susceptibility data), the $\rho(T)$ curves can be described by the Bloch–Grüneisen–Mott (BGM) formula

$$\rho(T) = (\rho_0 + \rho_\infty) + 4AT\left(\frac{T}{\theta_R}\right)^4 \times \int_0^{\theta_R/T} \frac{x^5\,\mathrm{d}x}{(\mathrm{e}^x - 1)\,(1 - \mathrm{e}^{-x})} - KT^3, \quad (1)$$

where the first term describes the scattering of conduction electrons on static defects in the crystal lattice (the residual resistivity ρ_0) as well as on disordered magnetic moments (the spin-disordered resistivity ρ_∞), the second one originates from the electron–phonon scattering (θ_R is the characteristic temperature of the order of the Debye temperature) and the third one stands for the interband s–d scattering. Fitting Eq. (1) to the experimental data yielded the following parameters: $\rho_0 + \rho_\infty = 25.4(1)$ $\mu\Omega$ cm, $\theta_R = 195.1(7)$ K, $A = 0.0971(8)$ $\mu\Omega$ cm/K, $K = -7.10(5) \times 10^{-8}$ $\mu\Omega$ cm/K^3 for $TbSn_2$, $\rho_0 + \rho_\infty = 19.6(2)$ $\mu\Omega$ cm, $\theta_R = 183.8(6)$, $A = 0.2702(7)$ $\mu\Omega$ cm/K, $K = -3.429(4) \times 10^{-7}$ $\mu\Omega$ cm/K^3 for $DySn_2$.

At low temperatures, the resistivity data manifest the magnetic orderings in the two compounds. For $TbSn_2$ as many as three distinct maxima at 27.8, 19.7 and 14.5 K are seen in the derivative $d\rho(T)/dT$, whereas for $DySn_2$ just one feature located at 12.6 K is observed (see the insets to Fig. 2).

3.3. Heat capacity

The results of the specific heat measurements of $TbSn_2$ and $DySn_2$ are presented in Fig. 3. For both compounds

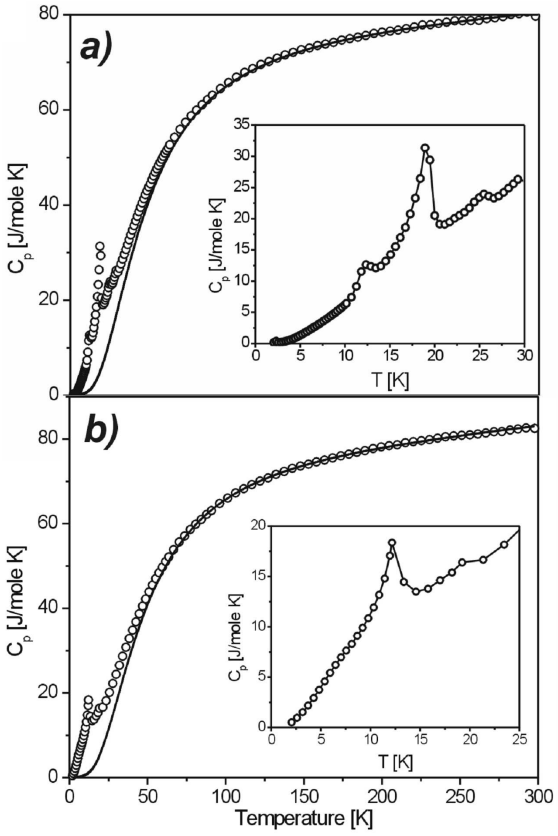

Fig. 3. Temperature dependences of the specific heat of $TbSn_2$ (a) and $DySn_2$ (b). The solid lines represent the sums of phononic and electronic contributions. The insets show the specific heat at the lowest temperatures studied.

the $C(T)$ curve has a usual sigmoid shape with superimposed peaks due to the magnetic phase transitions. For $TbSn_2$ three clear λ-like anomalies 13.1, 18.7 K and 26.9 K are seen, which match reasonably well with the features observed in the temperature dependence of the electrical resistivity. The latter originates from unknown spurious phase as its intensity is very low. Moreover, a less resolved singularity occurs at 2.5 K, i.e. at the position of the sharp peak in the $\chi(T)$ curve, which was attributed to the Tb_2O_3 impurity phase. For $DySn_2$ the main specific heat anomaly is apparent at 12.0 K, and this feature roughly corresponds to those established in the magnetic susceptibility and the electrical resistivity data. In addition, a small specific heat peak is seen at 19.5 K and a tiny hump in $C(T)$ at about 7 K. The latter anomaly may be related to minor yet discernible changes in the slopes of the $\chi(T)$ and $d\rho/dT(T)$ curves of the compound (*cf.* the insets to Fig. 1b and 2b). These two small features in $C(T)$ are likely due to small amounts of unknown magnetic impurities.

In order to analyze the magnetic contributions to the specific heat of $TbSn_2$ and $DySn_2$ it was assumed that the phononic and electronic contributions can be represented by the standard formula

$$C_{\mathrm{ph+el}} = 9R\left(\frac{T}{\Theta_{\mathrm{D}}}\right)^3 \int_0^{\frac{\Theta_{\mathrm{D}}}{T}} \frac{x^4 \mathrm{e}^x}{\left(\mathrm{e}^x - 1\right)^2}\,\mathrm{d}x + R\sum_i \frac{\left(\frac{\Theta_{\mathrm{Ei}}}{T}\right)^2 \mathrm{e}^{\frac{\Theta_{\mathrm{Ei}}}{T}}}{\left(\mathrm{e}^{\frac{\Theta_{\mathrm{Ei}}}{T}} - 1\right)^2} + \gamma T\,, \tag{2}$$

where Θ_{D} is the Debye temperature, Θ_{Ei} are the Einstein temperatures, γ is the electronic specific heat coefficient, and R stands for the gas constant. For the compounds investigated there are 3 acoustic modes (described by the first term) and 6 optical modes (described by the second term). For the sake of simplicity the optical modes were grouped into two triple-degenerated branches. Fitting Eq. (2) to the experimental data of the two compounds yielded the characteristic temperatures gathered in Table. It is worth noting that in both systems the average value over the characteristic temperatures Θ_{D} and Θ_{Ei} is of the same magnitude as the respective θ_R derived from the electrical resistivity data. The derived somewhat enhanced values of the electronic specific heat coefficient are typical of magnetically ordered rare-earth intermetallics.

TABLE

Characteristic temperatures (Θ_{D} — Debye temperature, Θ_{Ei} — Einstein temperatures) and the Sommerfeld coefficient γ representing the phononic and electronic contributions, respectively, to the specific heat of $TbSn_2$ and $DySn_2$.

	$TbSn_2$	$DySn_2$
Θ_{D} [K]	165.1(5)	164.6(5)
Θ_{E1} [K]	121.4(3)	121.2(2)
Θ_{E2} [K]	187.8(6)	185.7(6)
γ [mJ/(mol K^2)]	18.3(3)	20.9(3)

By subtracting $C_{\mathrm{ph+el}}(T)$ from the measured specific heat data purely magnetic contributions $C_{\mathrm{mag}}(T)$ were obtained (see Fig. 4). They are composed of the Schottky terms originating from splitting of the ground rare-earth multiplet in crystal field (CF) potential and terms due to magnetic orderings. The Schottky contribution can be quantified as

$$C_{\mathrm{Sch}} = \frac{R}{T^2}\left[\frac{\sum_{i=1}\delta_i^2 \mathrm{e}^{-\delta_i/T}}{\sum_{i=1}\mathrm{e}^{-\delta_i/T}} - \left(\frac{\sum_{i=1}\delta_i \mathrm{e}^{-\delta_i/T}}{\sum_{i=1}\mathrm{e}^{-\delta_i/T}}\right)^2\right] \tag{3}$$

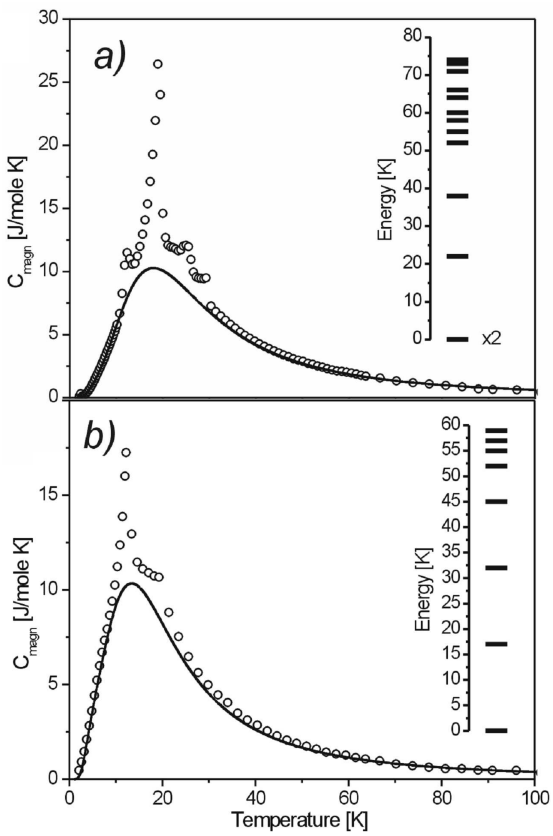

Fig. 4. Magnetic contributions to the specific heat of $TbSn_2$ (a) and $DySn_2$ (b). The solid lines represent the Schottky contributions. The insets display the corresponding crystal field levels scheme.

and δ_i are the energies of CF levels (in kelvins). As shown in Fig. 4, the best descriptions of $C_{\mathrm{mag}}(T)$ of $TbSn_2$ and $DySn_2$ were obtained with the CF levels splitting schemes given in the insets. For both compounds the overall CF splitting does not exceed 75 K, in line with the magnetic susceptibility and the electrical resistivity characteristics. In the case of the Tb-based stannide the ground state is a quasi doublet, separated from the other levels (all of them are singlets) by about 22 K. For the other compound studied all the split levels are doublets, as Dy^{3+} ion is the Kramers system. The first excited CF level is located about 17 K above the ground state.

4. Summary

The investigated compounds $TbSn_2$ and $DySn_2$ crystallise in the $ZrSi_2$-type structure, space group *Cmcm*. Both stannides order antiferromagnetically at low temperatures. The Néel points are likely 18.7 K in $TbSn_2$ and 12.0 K in $DySn_2$, as derived from the specific heat data. For $TbSn_2$, the additional anomaly in $C(T)$ occurring at 13.1 K, which is accompanied by the sharp feature in $\rho(T)$ at similar temperature, probably reflects some change in the magnetic structure. In turn, the weak resistivity and specific heat anomalies observed near 27 K are likely due to an unknown spurious phase. Such an interpretation of the experimental data for $TbSn_2$ seems supported by our preliminary neutron diffraction results (to be published in a separate paper).

The electrical resistivity measurements revealed metallic-like behaviour of both compounds. The Debye temperatures derived from $\rho(T)$ are about 190 K in both compounds, in reasonable agreement with the results of the analysis of the specific heat data. From the extracted Schottky contributions to $C(T)$ the models of crystal field level schemes in $TbSn_2$ and $DySn_2$ were developed, which are characterized by the total CF splitting less than 75 K, in line with the magnetic susceptibility and electrical resistivity data.

Acknowledgments

This work was partially supported by the National Scientific Network "Strongly correlated materials: preparation, fundamental research and applications".

References

[1] A. Iandelli, A. Palenzona, *AttiAccad. Naz. LinceiCl. Sci. Fis. Mat. Nat. Rend.* **40**, 623 (1966).

[2] L.C.J. Pereira, D.P. Rojas, J.C. Waerenborgh, *Intermetallics* **13**, 61 (2005).

[3] G. Venturini, A. Mesbah, *J. Alloys Compd.* **458**, 22 (2008).